

# Suppression of c-Met-Overexpressing Tumors by a Novel c-Met/CD3 Bispecific Antibody

This article was published in the following Dove Press journal:  
*Drug Design, Development and Therapy*

Lei Huang<sup>1</sup>  
Kun Xie<sup>1</sup>  
Hongwen Li<sup>1</sup>  
Ruiqin Wang<sup>1</sup>  
Xiaoqing Xu<sup>1</sup>  
Kaiming Chen<sup>1</sup>  
Hua Gu<sup>1</sup>  
Jianmin Fang<sup>1-3</sup>

<sup>1</sup>Laboratory of Molecular Medicine, Shanghai Key Laboratory of Signaling and Disease Research, School of Life Sciences and Technology, Tongji University, Shanghai 200092, People's Republic of China; <sup>2</sup>Department of Neurology, Tongji Hospital, Tongji University, Shanghai, People's Republic of China; <sup>3</sup>Biomedical Research Center, Tongji University Suzhou Institute, Suzhou, Jiangsu, People's Republic of China

**Introduction:** Overexpression of c-Met, or hepatocyte growth factor (HGF) receptor, is commonly observed in tumor biopsies and often associated with poor patient survival, which makes HGF/c-Met pathway an attractive molecular target for cancer therapy. A number of antibody-based therapeutic strategies have been explored to block c-Met or HGF in cancers; however, clinical efficacy has been very limited, indicating that blockade of c-Met signal alone is not sufficient. Thus, an alternative approach is to develop an immunotherapy strategy for c-Met-overexpressing cancers. c-Met/CD3 bispecific antibody (BsAb) could bridge CD3-positive T lymphocytes and tumor cells to result in potent tumor cell killing.

**Materials and Methods:** A bispecific antibody, BS001, which binds both c-Met and CD3, was generated using a novel BsAb platform. Western blotting and T cells-mediated killing assays were utilized to evaluate the BsAb's effects on cell proliferation, survival and signal transduction in tumor cells. Subcutaneous tumor mouse models were used to analyze the in vivo anti-tumor effects of the bispecific antibody and its combination therapy with PD-L1 antibody.

**Results:** BS001 showed potent T-cell mediated tumor cells killing in vitro. Furthermore, BS001 inhibited phosphorylation of c-Met and downstream signal transduction in tumor cells. In A549 lung cancer xenograft model, BS001 inhibited tumor growth and increased the proportion of activated CD56<sup>+</sup> tumor infiltrating lymphocytes. In vivo combination therapy of BS001 with Atezolizumab (an anti-programmed cell death protein1-ligand (PD-L1) antibody) showed more potent tumor inhibition than monotherapies. Similarly, in SKOV3 xenograft model, BS001 showed a significant efficacy in tumor growth inhibition and tumor recurrence was not observed in more than half of mice treated with a combination of BS001 and Pembrolizumab.

**Conclusion:** c-Met/CD3 bispecific antibody BS001 exhibited potent anti-tumor activities in vitro and in vivo, which was achieved through two distinguished mechanisms: through antibody-mediated tumor cell killing by T cells and through inhibition of c-Met signal transduction.

**Keywords:** c-Met, bispecific antibody, lung cancer, ovarian cancer, checkpoint antibody

## Introduction

c-Met is the receptor for hepatocyte growth factor (HGF) and belongs to the receptor tyrosine kinase (RTK) family proteins. c-Met is often aberrantly expressed and constitutively activated in many types of human cancers such as in lung, ovarian, and liver cancers, suggesting that c-Met is a promising therapeutic target for cancers.<sup>1-3</sup> The HGF/c-Met signaling pathway plays a key role in growth factor-stimulated proliferation, epithelial-mesenchymal transition-dependent metastasis, and AKT-regulated survival.<sup>4,5</sup> HGF forms a tight complex with c-Met and initiates dimerization of the receptor and phosphorylation of multiple tyrosine residues in

Correspondence: Hua Gu  
Tel +86-21-6598-2867  
Email gu\_hua@tongji.edu.cn

Jianmin Fang  
Tel +86-21-6598-2878  
Email jfang@tongji.edu.cn

the intracellular kinase domain of c-Met, thereby activating multiple signal cascades in tumor cells. These downstream signals within the cell are closely related to cell proliferation, invasion and metastasis.<sup>6</sup>

Several kinase inhibitor and monoclonal antibody-based therapeutics have been tested in clinical studies to inhibit the HGF/c-Met signal transduction by blocking the binding of HGF to c-Met or for direct targeting of c-Met on the cell surface.<sup>7–11</sup> Conventional bivalent antibodies often cause c-Met auto-activation due to antibody-mediated c-Met dimerization. In order to avoid antibody-induced c-Met activity, several approaches have been developed. Emibetuzumab, a full-length antibody against c-Met, can inhibit c-Met signaling by inducing endolysosomal-mediated degradation of c-Met, thus diminishing c-Met signaling.<sup>12</sup> Onartuzumab, a c-Met-targeted monovalent antibody, can block HGF/c-Met interaction while avoiding c-Met activation due to its monovalent nature.<sup>13,14</sup> Despite the success of these antibodies in pre-clinical models, overall, clinical development of c-Met-targeting antibody therapeutics has been very challenging. Several HGF antibodies have also been evaluated in clinical trials. Rilotumumab<sup>15</sup> and ficlatuzumab<sup>16</sup> are two monoclonal antibodies against HGF. They inhibit HGF/c-Met binding, but both failed to improve clinical outcomes. Taken together, it seems that sole inhibition of HGF/c-Met signal is likely insufficient to achieve clinical efficacy. New strategies are needed to target c-Met to exploit it as a tumor marker.

T-cell-dependent bispecific (TDB) antibodies could effectively trigger the cytotoxicity of effector cells toward tumor cells.<sup>17,18</sup> A c-Met targeting, T-cell mediating BsAb has a potential to generate therapeutic benefit to c-Met over-expressing tumors. Among T-cell mediating bispecific antibodies, blinatumomab is a BsAb with two single-chain variable fragment (scFv) targeting CD3 and CD19, respectively, and has gained market approval for treatment of CD19 positive leukemia.<sup>19</sup> However, blinatumomab requires continuous intravenous infusion due to its short half-life, which has severely limited its clinical use. It is apparent that a BsAb with a longer half-life time would have great advantages.

In this study, we generated a novel bispecific antibody, named BS001. This BsAb has a monovalent, asymmetric structure to avoid c-Met auto-activation and an IgG1 Fc to extend drug half-life time. It specifically binds to c-Met and CD3, eliciting the T-cell mediating tumor cell killing. Both in vitro and in vivo results demonstrated its therapeutic effects against c-Met-positive tumor models, and,

moreover, can show increased therapeutic benefits in combination with PD-1/PD-L1 antibodies.

## Materials and Methods

### Clinical Samples

Human lung, ovarian, breast cancer samples were obtained from Tongji Hospital, Shanghai, China with written informed consent from the donors. The study was performed according to the Declaration of Helsinki and was approved by the Institutional Ethics Committee of Tongji Hospital in Shanghai, China. Excised tumor tissues were paraffin-embedded and sectioned for immunohistochemistry staining of c-Met antibody (ab51067; Abcam, Cambridge, UK). Human peripheral blood was obtained from Changhai Hospital Blood Center (Shanghai, China) with written informed consent from the donors.

### Database Search

*c-Met* gene expression in lung adenocarcinoma, lung squamous cell carcinoma, ovarian cancers, and their respective normal tissues was analyzed using the TCGA database,<sup>20</sup> represented as  $\log_2(\text{Transcripts Per Million}+1)$ . Box-whisker plots showing the expression of c-Met without restrictions in stage, gender, race or grade were analyzed using UALCAN.<sup>21</sup> Overall survival (OS) of lung adenocarcinoma and ovarian cancer patients was analyzed using KMplotter.<sup>22</sup> c-Met-high and c-Met-low expression groups were compared without restrictions in stage, gender, race or grade in the above two tumor types. *P* value was calculated in the Kaplan–Meier curves.

### Cell Lines and Cell Culture

A549, SKOV3, HepG2, MDA-MB-231, and MDA-MB-468 cells were purchased from American Type Culture Collection (Rockville, MD, USA) and cultured in Dulbecco's modified Eagle medium (Hyclone, Waltham, MA, USA) supplemented with 10% fetal bovine serum (Cegrogen, Stadtallendorf, Germany), 100 U/mL penicillin (Gibco, Waltham MA, USA), and 100 µg/mL streptomycin (Gibco, Waltham MA, USA) at 37°C and 5% CO<sub>2</sub>. Peripheral blood mononuclear cell (PBMC) from donors were cultured in RPMI 1640 (100 U/mL penicillin, 100 µg/mL streptomycin, 10% heated fetal bovine serum, 300 U/mL IL2; Gibco, Waltham MA, USA). Chinese hamster ovary (CHO) cells were cultured in a serum-free medium according to our previous report.<sup>23</sup> All Cell lines were tested for no contamination.



## Reverse Transcription-Polymerase Chain Reaction (RT-PCR)

Total RNA was extracted from A549, SKOV3, HepG2, and MDA-MB-468 cells using TRIzol reagent (Solarbio, Beijing, China) and reverse-transcribed with Reverse Transcription System (Solarbio, Beijing, China). Quantitative PCR was performed on a LightCycler96 instrument (Roche) using SYBR Green PCR Kit (Solarbio, Beijing, China). The qPCR profile of the reaction was 95°C for 5 min, followed by 40 cycles of denaturation at 95°C for 10 s, annealing at 60°C for 10 s, and extension at 72°C for 30 s. The primers used were as follows: *c-Met*, forward (5' -ACA GTG GCA TGT CAA CAT CGC T-3') and reverse (5' -GCT CGG TAG TCT ACA GAT TC-3'); GAPDH, forward (5' -CAA TGA CCC CTT CAT TGA CC-3') and reverse (5' -GAC AAG CTT CCC GTT CTC AG-3'). GAPDH mRNA expression was measured as an endogenous control, and MDA-MB-468 cells were as the calibrator sample.

## Immunofluorescence Staining

A549, SKOV3, HepG2, and MDA-MB-468 cells were coated on glass bottom plates before staining, then fixed with 4% paraformaldehyde for 30 min, blocked with BSA buffer and stained with c-Met antibody (ab51067, Abcam, Cambridge, UK). For tumor immunofluorescence staining, samples were fixed immediately in 4% paraformaldehyde overnight at 4°C and stained with CD3 antibody (ab16669, Abcam, Cambridge, UK), PD-L1 antibody (ab205921, Abcam, Cambridge, UK) and Alexafluor-488/594 labeled antibody (Molecular Probes, Eugene, USA).

## Western Blot Analyses

Cells were lysed in RIPA buffer (Solarbio, Beijing, China), supplemented with protease (B14001; Bimake, Houston, TX, USA) and phosphatase inhibitor cocktails (B15001; Bimake, Houston, TX, USA). The protein concentrations were measured by BCA Protein Assay Kit (Beyotime, Shanghai, China) and heat denatured in the presence of reducing agent. A total of 20 µg protein were subjected to 10% SDS-PAGE (EpiZyme, Shanghai, China), and transferred to polyvinylidene fluoride (PVDF) membranes (Millipore). Membranes were blocked in 5% bovine serum albumin and probed with primary antibodies overnight at 4°C, and then incubated with the relevant secondary antibody for 2 h at room temperature. Bands were visualized by Electrochemiluminescence (ECL) and

quantified using ImageJ software (NIH, Bethesda, MD, USA). Protein bands were quantified relative to the loading control (GAPDH).

The receptor phosphorylation assay was performed using A549 cell ( $5 \times 10^3$  cells/well) and a dose-gradient curve of BS001 for 8 h or JNJ-38,877,605 for 2 h or the combined treatments.<sup>24</sup> Then, the cells were supplemented with 100 ng/mL HGF, incubated for 30 min, and then lysed. This assay was also performed with the parental monovalent c-Met antibody produced by ourselves.<sup>25</sup> The antibodies used in Western blotting included c-Met (ab51067, Abcam, Cambridge, UK), phospho-c-Met (3077S), MAPK (4696S), phospho-MAPK (4376S), AKT (4691S), phospho-AKT (13038S) from Cell Signaling Technology (Boston, MA, USA), STAT3 (A1192, Abclonal, Wuhan, China), phospho-STAT3 (AP0070; Abclonal, Wuhan, China), GAPDH (A5028, Bimake, Houston, TX, USA), anti-rabbit-IgG-HRP (A120-111P, Bethyl Laboratories, Montgomery, TX, USA), and anti-mouse-IgG-HRP (A90-131P, Bethyl Laboratories, Montgomery, TX, USA).

## Construction and Expression of Bispecific Antibody (BS001)

For the construction of c-Met/CD3 bispecific antibody BS001, the variable regions of antibody heavy and light chains of an anti-c-Met antibody were cloned from a murine hybridoma cell line generated in our laboratory;<sup>25</sup> the anti-CD3 single-chain antibody sequence was based on OKT3 scFv (GenBank: AND42858.1). The monovalent asymmetric bispecific antibody includes three chains (Figure 2A) constructed using the polymerase chain reaction (PCR). To express BS001, the light and heavy expression vectors were co-transfected into CHO cells for stably expression. The recombinant antibodies were purified by Protein A affinity chromatography (Thermo Scientific, Waltham, MA, USA) and followed by gel filtration chromatography. The antibody was analyzed by analytic size exclusion chromatography in a Zenix SEC-300 column (Sepax Technologies, Newark, PA, USA) using an Agilent 1100 HPLC system (Agilent Technologies, Santa Clara, CA, USA). Protein samples were subjected to 10% SDS-PAGE (EpiZyme, Shanghai, China) and dyed with Coomassie brilliant blue.

## Antibody Ligand Binding

Lung cancer cell line A549, ovarian cancer cell line SKOV3, and breast cancer cell line MDA-MB-231 ( $1 \times 10^6$  cells/mL,

100  $\mu$ L), human PBMC, CD3<sup>+</sup>T, CD4<sup>+</sup>T and CD8<sup>+</sup>T ( $1 \times 10^7$  cells/mL, 100  $\mu$ L) were separately treated on ice for 1 h with indicated concentration (0.0001 to 100  $\mu$ g/mL) of BS001 and the monovalent c-Met antibody, then for 30 min with IgG Fc-APC (409,306, Biolegend, San Diego, CA, USA) and analyzed by fluorescence-activated cell sorting (FACSCalibur, BD Biosciences, San Jose, CA, USA). Data were analyzed using FlowJo7.6.2 software (TreeStar, Inc., Ashland, OR, USA).

## PBMC/Pan-T Isolation

PBMCs were separated from the blood of healthy donors or mice using lymphocyte separation medium (Tbdscience, Tianjin, China). Human CD3<sup>+</sup>T cells were microbeads-isolated from PBMC using a pan T cell isolation kit (130-096-535; Miltenyi Biotec, Teterow, Germany) by negative selection according to the manufacturer's protocol. CD4<sup>+</sup>T or CD8<sup>+</sup>T cells were isolated using positive selection (130-096-533, 130-045-201; Teterow; Miltenyi Biotec). The purified T cells were maintained in the presence of IL-2 (300 U/mL; Peprotech, NJ, USA) for up to 2 weeks.

## In vitro Co-Culture and Killing Assay

A549 and SKOV3 cancer cells were co-cultured with indicated concentrations (0–10  $\mu$ g/mL) of BS001 for 30 min and then PBMC cells. After 1 h, unbound cells were aspirated together with supernatant for subsequent FACS analysis using FITC-CD3 (561,807), APC-CD4 (561,841), and PE-CD8 (561,950) from BD Pharmingen (San Diego, USA). In vitro cytotoxicity assays, A549, SKOV3, and MDA-MB-231 cancer cells were co-cultured with PBMC (E:T=10:1) in 96-well plates (Corning, NY, USA), and indicated concentrations of BS001 or control parental anti-c-Met antibody (monovalent) were added. The plate was incubated at 37°C for 8 h, and the levels of released LDH were detected by CytoTox 96 (Promega, Madison, WI, USA) and calculated.<sup>26</sup> There are four cell-culture replicates for each condition and three donors of each experiment. Cytotoxicity was calculated following the formula: (Experiment LDH - Effector spontaneous LDH - Target spontaneous LDH)/(Target maximum LDH-Target spontaneous LDH).

Microbeads-isolated CD3<sup>+</sup>T and SKOV3 cells were co-cultured with 1  $\mu$ g/mL BS001 antibody and photographed after 1 h. BsAb-mediated CD3<sup>+</sup>T or CD8<sup>+</sup>T cytotoxicity of A549 and SKOV3 cells with 1  $\mu$ g/mL BS001 antibody was measured as described assays (E:T=1:1). PerCP-Cy5.5-CD69 (560,738, BD Pharmingen, San Diego, USA)

and V450-Interferon (IFN)- $\gamma$  (562,988, BD Pharmingen, San Diego, USA) was used for co-cultured T cell activation and secretion detection.

## Xenograft Mouse Models

All the procedures relating to animal care, handling, and treatment were performed according to the Directive 2010/63/EU in Europe approved by the Animal Research Ethics Committee at Tongji University (No. TJLAC-018-032). Nude mice were obtained from the Shanghai SLAC Laboratory Animal Co., Ltd. (Shanghai, China) and fed in a pathogen-free environment.

On day 0,  $5 \times 10^6$  A549 cells and  $5 \times 10^6$  human PBMCs were pre-mixed and inoculated in the right flank of the 6- to 8-week-old nude mice (100  $\mu$ L/mouse).<sup>27</sup> One day after inoculation, the mice were randomized into groups (n = 6/group) and then injected intravenously with different concentration of BS001 (0, 4, 10, 25 mg/kg) in 100  $\mu$ L of PBS per mouse every 3 days. After 18 days under administration, animals were euthanized and tumors were collected, dissected into small pieces, and incubated with 0.1% Collagenase Type I (17,100-017; Invitrogen, Waltham MA, USA) supplemented Hanks' balanced salt solution medium (2,005,368; Gibco, Waltham MA, USA) for 20 min at 37°C. Primary cells were harvested, washed, resuspended in HBSS containing 1% bovine serum albumin, and stained with FITC-CD3 (561,807), PE-CD8 (561,950), PE-Cy7-CD25 (557,741), BV510-CD56 (563,041) from BD Pharmingen (San Diego, USA) and analyzed by FACS.

In drug combination experiments, for A549 models,  $5 \times 10^6$  cells were injected subcutaneously into the flanks (100  $\mu$ L/mouse). PBMCs ( $5 \times 10^7$  cells/mouse) were injected in the tail vein (n = 6/group) when all tumors reached the size of 50 to 150 mm<sup>3</sup> (no PBMC injection in vehicle group). Mice were randomly divided into 4 groups with the similar mean tumor size and treated with PBS, BS001 antibody (10 mg/kg), PD-L1 antibody (5 mg/kg; Atezolizumab, Roche, Mannheim, Germany), or their combination (BS001 and PD-L1 antibody) per mouse twice a week for a total of five doses. Mouse body weight was determined with an electronic scale. On day 7 and day 14 of BS001 and anti-PD-L1 combination experiment in A549 model, peripheral blood of three samples from each group was obtained and AST/ALT levels in serum were measured with detection kit (C0010-2, C009-2; Nanjing Jiancheng Biotec, China).

Similarly, for SKOV3 model ( $5 \times 10^6$  cells/mouse, E: T=10:1), mice were treated with vehicle (PBS), BS001 antibody (10 mg/kg), or BS001 with PD-1 antibody (10 mg/kg; Pembrolizumab, Merck & co., NJ, USA) twice a week. Tumors were measured with a caliper on the indicated days and tumor volume ( $\text{mm}^3$ ) was calculated using the following formula:  $(\text{length} \times \text{width}^2)/2$ . Tumor volume was analyzed by two-way ANOVA analysis (GraphPad Prism v6, La Jolla, CA, USA).

## Statistical Analysis

Statistical analysis was performed using Prism 6 (GraphPad Software Inc., La Jolla, CA, USA). Results are shown as the means  $\pm$  SEM, which were calculated from at least triplicate technical or biological replicates. Statistical significance was analyzed by unpaired two-tailed *t* test unless otherwise indicated. Differences were considered significant at  $p < 0.05$ .

## Results

### c-Met Gene Expression in Tumor Specimens and Cell Lines

To quantitate c-Met expression in tumor biopsies, a panel of carcinoma tissues and adjacent tissues from lung adenocarcinoma, lung squamous cell carcinoma, and ovarian cancer patients were stained using a c-Met antibody. Immunohistochemistry analysis of those specimens revealed that all tumor cells were c-Met positive at 1–3<sup>+</sup> scores, whereas cells in the adjacent tissues were negative, suggesting that c-Met overexpression is tumor-cell specific (Figure 1A, Figure S1A). Consistently, RNA-seq data at the TCGA also showed that the transcriptional levels of *c-Met* gene were higher in lung adenocarcinoma, lung squamous cell carcinoma, and ovarian cancer compared to that in their respective normal tissues (Figure 1B). The Kaplan–Meier curves suggested a trend that a higher c-Met expression level is related to a poorer patient survival in lung adenocarcinoma ( $p = 0.02$ ) and ovarian cancer ( $p = 0.023$ ) (Figure 1C).

We also identified several tumor cell lines that express *c-Met* mRNA at increased levels (1.5–2.84-fold increase in copy number by RNA-seq) than c-Met-negative MDA-MB-468 cell line (Figure 1D). c-Met expression in these cells were further confirmed at the protein level by Western blotting (Figure 1E) and immunofluorescence (Figure S1B). In flow cytometry analysis, A549, SKOV3, and HepG2 cells

showed positive staining with c-Met antibody (Figure 1F) and were chosen for further analysis.

### Expression and Activities of a c-Met/CD3 Bispecific Antibody

To generate a bispecific antibody for c-Met-targeted immunotherapy, we constructed a novel BsAb, BS001, that contains an anti-CD3 scFv attached to the N-terminus of the heavy chain of a monovalent, single-arm, anti-c-Met antibody (Figure 2A). This asymmetric antibody was expressed in CHO cells with a good yield in transient expression as well as stable cell lines. After protein A and gel filtration chromatographies, the bispecific antibody reached over 99% in purity as assessed by size exclusion HPLC (Figure 2B). SDS-PAGE analysis confirmed the correct molecular weights of three respective bands of the antibody in both reducing and non-reducing gels (Figure 2C). In flow cytometry analyses, BS001 showed high binding activity to c-Met-positive A549 and SKOV3 cells but not to c-Met-negative MDA-MB-231 cells (Figure 2D). BS001 could bind to human PBMC isolated from different donors, and dose-dependently bind to CD3<sup>+</sup>T (both CD4<sup>+</sup>T and CD8<sup>+</sup>T), consistent with the expected biological activity of the anti-CD3 scFv in this antibody (Figure 2E, Figure S1C). Therefore, this bispecific antibody has binding activities to both c-Met and CD3 on cell surface.

### BS001-Mediated Tumor Cell Killing by T-Cells

To evaluate whether BS001 bispecific antibody can trigger effector cell-mediated cytotoxicity to tumor cells, A549 or SKOV3 tumor cells were co-cultured with human PBMC. The tumor-killing effect was further quantitated, in which increasing concentrations of BS001 resulted in increased tumor cell lysis in a dose-dependent manner (Figure 3A). This effect was not seen or minimal in c-Met-negative or very low expression tumor cells, such as MDA-MB-231 cells (Figure 3B). To make a clear elucidation, addition of BS001 antibody to the co-culture systems caused the cells from PBMC compartment (presumably CD3<sup>+</sup>T cells) became attached to tumor cells at bottom of culture dishes, subsequently death of tumor cells in the co-cultures (Figure 3C). The numbers of suspended PBMC (not attached to tumor cells) cells in the cultures decreased with increasing concentrations of the bispecific antibody as shown by FACS (Figure S2B). Similarly, BS001-mediated cytotoxicities were also shown in the co-culture systems of tumor cells and purified T lymphocytes

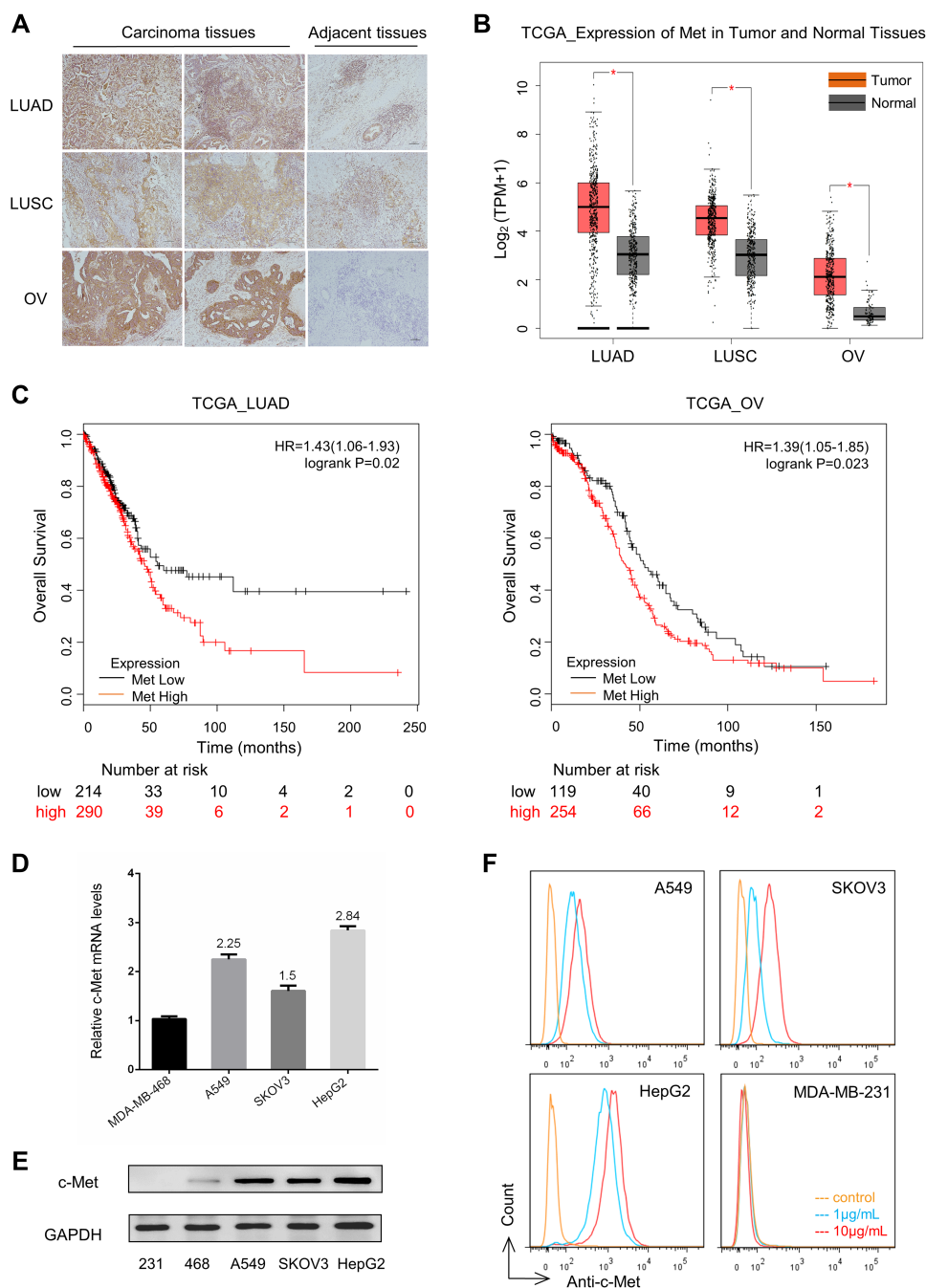


**Figure 1** *C-Met* gene expression in tumor specimens and cell lines.

**Notes:** (A) *c-Met*-positive reactivity with tumor specimens (2 images from different regions in the same tumor) and adjacent tissues by immunohistochemistry, including patients with LUAD, LUSC, and OV. Representative tumor biopsies (2LUAD, 1LUSC, 3OV) were also shown in Figure S1A. Bar: 100μm; (B) *c-Met* gene transcriptional levels analyses in LUAD, LUSC, OV and their respective normal tissues at the TCGA database; (C) Kaplan–Meier curves showing the effect of *Met* expression level on the survival of patients with LUAD ( $p = 0.02$ ) and OV ( $p = 0.023$ ); (D) *c-Met* gene transcriptional levels were detected by RT-PCR in MDA-MB-468, A549, SKOV3, and HepG2 cells. MDA-MB-468 expression level was used as a control, three replicates for each group; (E) *c-Met* protein expression was detected in human cell lines: MDA-MB-231, MDA-MB-468, A549, SKOV3, and HepG2 with *c-Met* antibody (Abcam) by Western blotting analysis. GAPDH expression was used as an internal control; (F) Flow cytometry analyses of *c-Met* binding to A549, SKOV3, HepG2, and MDA-MB-231 cells with *c-Met* antibody (Abcam). MFI values with 1μg/mL *c-Met* antibody of A549, SKOV3, HepG2 and MDA-MB-231 were respectively 835, 550, 1146 and 25.

**Abbreviations:** LUAD, lung adenocarcinoma; LUSC, lung squamous cell carcinoma; OV, ovarian cancer; TCGA, The Cancer Genome Atlas; MFI, mean fluorescence intensity.

(Figure 3D, Figure S2C). Thus, this bispecific antibody can effectively direct CD3-positive cells to *c-Met*-expressing tumor cells (Figure 3E), and killing of tumor cells. To figure out the possible killing mechanism on different tumor cells,

co-culturing A549 or SKOV3 cells with purified T cells from individual donors was shown that BS001 promoted CD69 expression (an early activation marker) and IFN- $\gamma$  secretion within CD3<sup>+</sup>T cells (Figure 3F, Figure 3G).



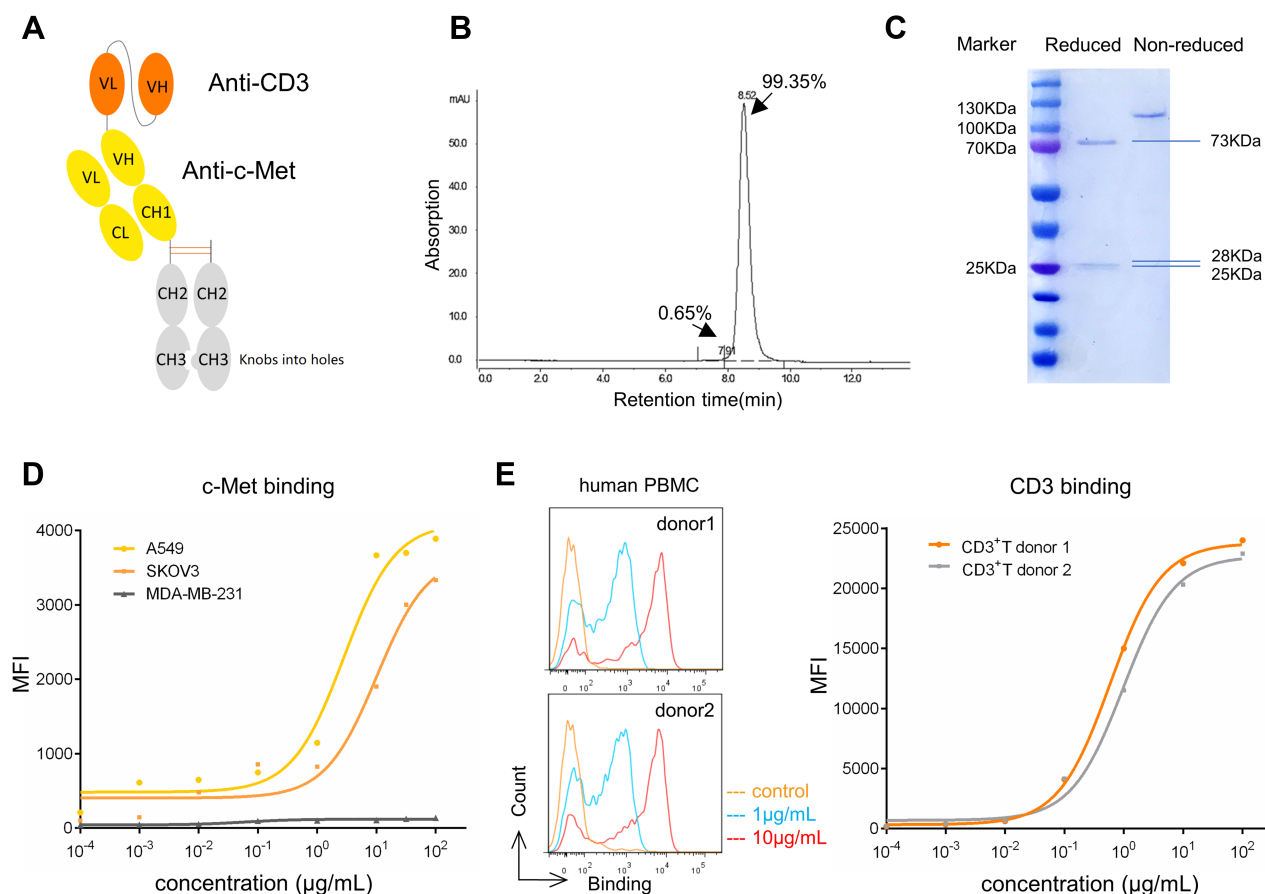


**Figure 2** C-Met/CD3 (BS001) antibody expression and activities.

**Notes:** (A) Structure diagram of c-Met/CD3 bispecific antibody; (B) In size-exclusion HPLC, purified BS001 showed a single peak with a retention time consistent with its expected molecular weight of 125 kDa. Purity: 99.35%; (C) Integrity of the purified BS001 protein analyzed by SDS-PAGE. Under denaturing, reducing and non-reducing conditions, three chains of BS001 were observed at the expected size of 75, 28, and 26 kDa; (D) Flow cytometry analyses of BS001 in c-Met binding to A549, SKOV3, and MDA-MB-231; (E) Flow cytometry analyses of BS001 in CD3 binding to PBMC and human CD3<sup>+</sup>T from 2 donors.

**Abbreviations:** HPLC, high-performance liquid chromatography; SDS-PAGE, sodium dodecyl sulfate-polyacrylamide gel electrophoresis; PBMC, peripheral blood mononuclear cell; MFI, mean fluorescence intensity.

## BS001 Inhibits c-Met Phosphorylation and Downstream Signal Transduction

After determining that BS001 bispecific antibody induces T-cell mediated tumor killing, we tested whether BS001 with monovalent nature could block the interaction between HGF and c-Met, thus, potentially inducing tumor cell apoptosis. When increasing concentrations of BS001 protein was added to cultured A549 cells and stimulated by HGF, BS001 showed dose-dependent inhibition on HGF-induced phosphorylation of c-Met. To determine whether inhibition of receptor phosphorylation affect downstream signal transduction of c-Met, phospho-AKT, phospho-STAT3, and phospho-MAPK in A549 cells treated with BS001 were measured. BS001 potentially inhibited HGF-induced phospho-AKT, phospho-MAPK, and phospho-STAT3 (Figure 4A, Figure S1G). Furthermore, BS001 has an equivalent inhibition on c-Met phosphorylation

to a small-molecule inhibitor, JNJ-38,877,605 both at 0.5  $\mu$ M (Figure 4B). Moreover, the combined treatment of 0.5  $\mu$ M BS001 and 0.5  $\mu$ M JNJ-38,877,605 showed higher inhibition of phospho-c-Met and phospho-STAT3 than monotherapy in vitro (Figure 4C, Figure 4D). These data suggested that blocking the HGF-stimulated c-MET pathway by BS001 is an effective targeted therapy, providing possibilities with combined use of the macromolecule and small molecule.

## BS001 Inhibits Tumor Growth in Xenograft Models

The in vivo anti-tumor efficacy of BS001 was evaluated in adoptive transfer xenograft tumor models. A549 cells and PBMC were mixed and implanted into immunodeficient nude mice as demonstrated in the methods. As shown in Figure 5A, BS001 inhibited tumor growth in dose-

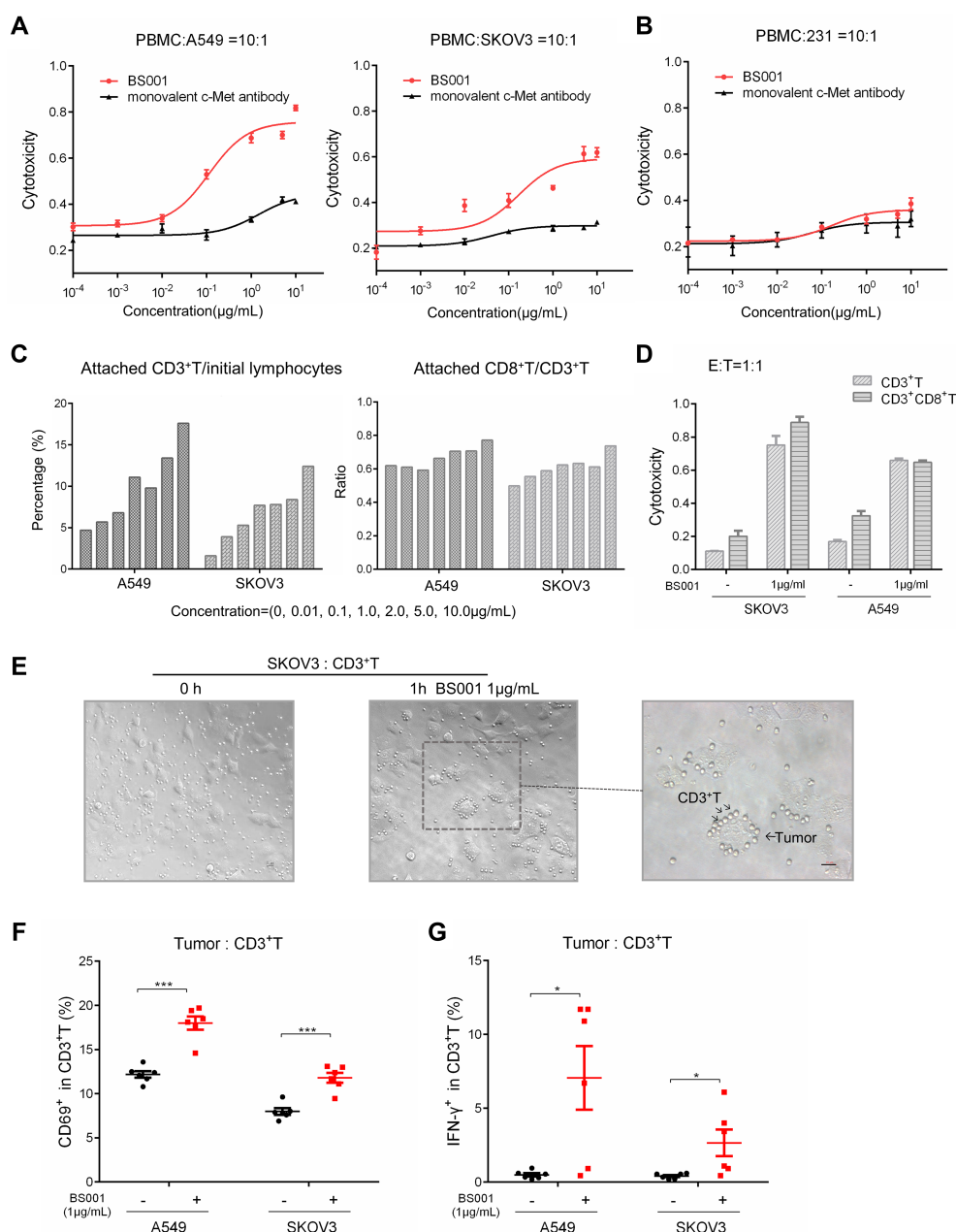


**Figure 3** BS001-mediated T-cell engagement and killing of tumor cells.

**Notes:** (A and B) PBMC killing activity on A549, SKOV3 and MDA-MB-231 cells (E:T=10:1) mediated by BS001 and control parental anti-c-Met antibody (monovalent) at doses of 0.0001–10  $\mu\text{g/mL}$  was analyzed by LDH detection. The results were shown as mean  $\pm$  SEM; (C) FACS analyses for the PBMC before the addition to the attached tumor cells as “initial lymphocytes” were shown in Figure S2A. Percentage increases of attached CD3<sup>+</sup>T (initial ratio–test ratio) and ratios of CD8<sup>+</sup>T/CD3<sup>+</sup>T cells attached to tumors after co-culture at doses of 0–10  $\mu\text{g/mL}$  BS001 were calculated with the following formula:  $\text{CD8}^+ / (\text{initial ratio} - \text{test ratio}) / \text{CD3}^+ / (\text{initial ratio} - \text{test ratio})$ ; (D) CD3<sup>+</sup>T or CD8<sup>+</sup>T cytotoxicity of A549 and SKOV3 cells mediated by 1  $\mu\text{g/mL}$  BS001. The percentage of cytotoxicity was calculated with the following formula:  $(\% \text{ of tumor cells in effectors plus BS001}) - (\% \text{ of tumor cells in effectors})$ ; (E) Co-culture of SKOV3 and microbeads-sorted CD3<sup>+</sup>T cells (E:T=1:1) with 1  $\mu\text{g/mL}$  BS001 for 1 h in 6-well plate. Photograph showed BS001-mediated binding of tumor cells and T cells (plotted by the arrows); (F) CD69 expression in CD3<sup>+</sup>T cells with or without 1  $\mu\text{g/mL}$  BS001 treatment was detected by FACS. N = 6 donors for each group. Data shown represent the CD69 expression level of CD3<sup>+</sup>T cells from individual donors.  $^{***}p < 0.001$  by unpaired two-tailed t-test; (G) IFN- $\gamma$  protein levels in CD3<sup>+</sup>T cells with or without 1  $\mu\text{g/mL}$  BS001 treatment was detected by FACS. N = 6 donors for each group. Data shown represent the IFN- $\gamma$  expression level of CD3<sup>+</sup>T cells from individual donors.  $^*p < 0.05$  by unpaired two-tailed t-test.

**Abbreviations:** FACS, fluorescence-activated cell sorting; LDH, lactate dehydrogenase; IFN- $\gamma$ , interferon- $\gamma$ .

dependent manner compared to that of the control group on day 18 ( $p < 0.01$ ). At 4 mg/kg BS001, tumor growth was inhibited by approximately 50%, while 10 or 25 mg/kg inhibited tumor growth by nearly 100%. Flow

cytometry of isolated tumors showed that tumor infiltrated CD3<sup>+</sup>CD8<sup>+</sup>T cells in the 4 and 10 mg/kg groups were higher than those in the control group, indicating that the bispecific antibodies effectively recruited and maintained

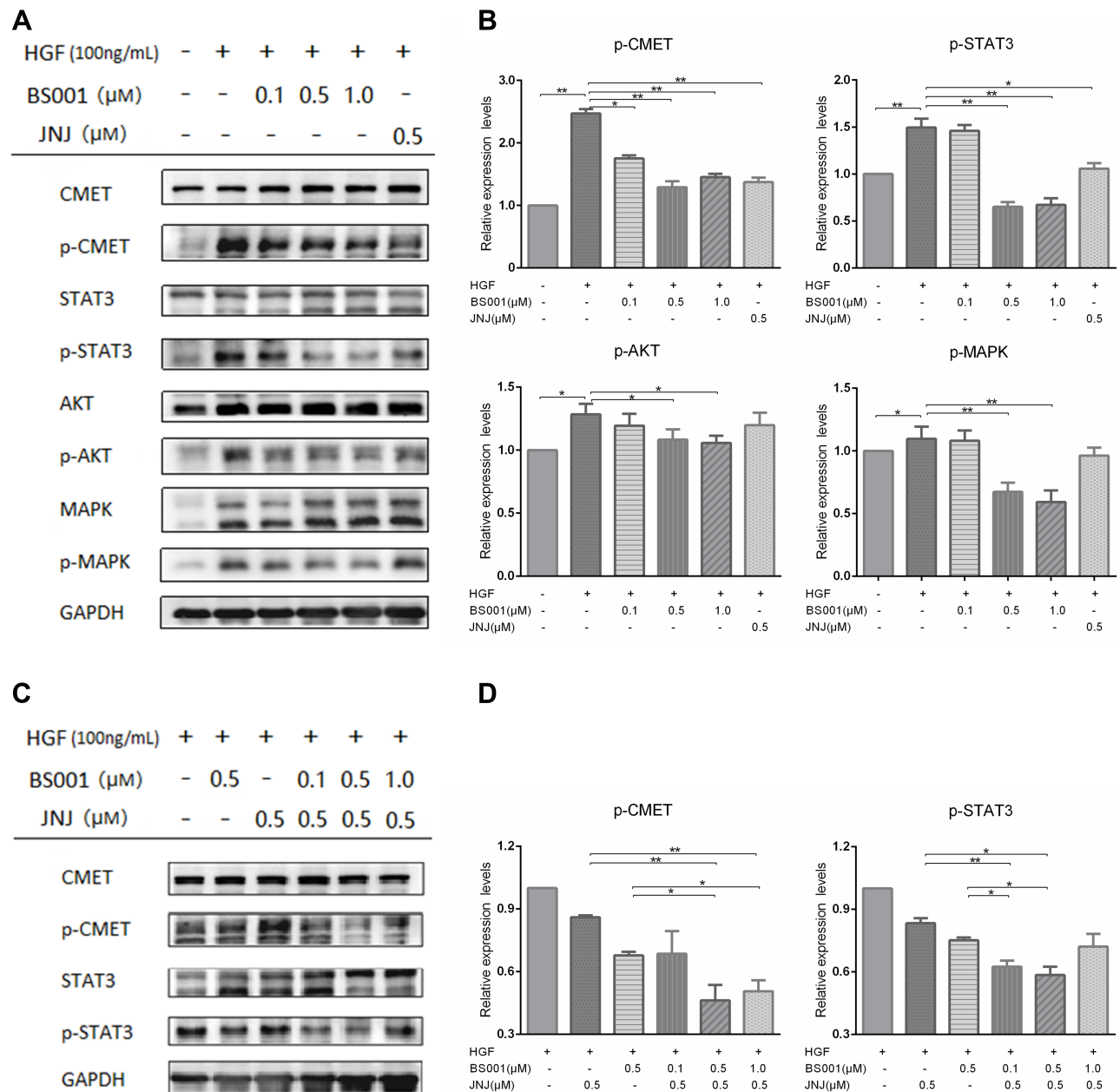


**Figure 4** BS001 inhibits HGF-mediated c-Met phosphorylation and downstream signal transduction.

**Notes:** (A) A549 cells were treated with the indicated concentrations of BS001 for 8 h or JNJ-38,877,605 for 2 h, and then stimulated with or without HGF (100 ng/mL) for 30 min. Total cell lysates were evaluated by Western blotting using indicated antibodies. GAPDH expression was used as an internal control, N = 3 for each group; (B) Analyses of inhibition on the phosphorylation of c-Met and downstream signal by dosages of BS001 and JNJ-38,877,605. The results were shown as mean  $\pm$  SEM. \* $p$  < 0.05, \*\* $p$  < 0.01, vs HGF group by unpaired two-tailed t-test; (C) A549 cells were treated with the indicated concentrations of BS001 for 8 h, JNJ-38,877,605 for 2 h or the combined groups, and then stimulated with HGF (100 ng/mL) for 30 min. Total cell lysates were evaluated by Western blotting using indicated antibodies. GAPDH expression was used as an internal control, N = 3 for each group; (D) Analyses of inhibition on the phosphorylation of c-Met and downstream STAT3 signal by dosages of BS001, JNJ-38,877,605 and the combined groups. The results were shown as mean  $\pm$  SEM. \* $p$  < 0.05, \*\* $p$  < 0.01.

**Abbreviations:** HGF, hepatocyte growth factor; STAT3, signal transducer and activator of transcription 3; AKT, v-Akt gene expression protein, also referred to as PKB (Protein kinase B); MAPK, mitogen-activated protein kinase; JNJ-38,877,605, a c-Met inhibitor.

T cells (Figure 5B, Figure S3A). Flow cytometry analyses also showed that ratios of CD56<sup>+</sup>T lymphocytes, which indicates T cell activation, increased in the 4 and 10 mg/kg of BS001 groups (Figure 5C, Figure S3BD), suggesting that the bispecific antibody promotes an immune response

against the tumors. On the other hand, increased PD-L1 expression was observed in A549 tumor tissues treated with the BS001 (Figure 5DE), a tumor cell response that may compromise activated T cells by inducing PD-1 signal in T lymphocytes.

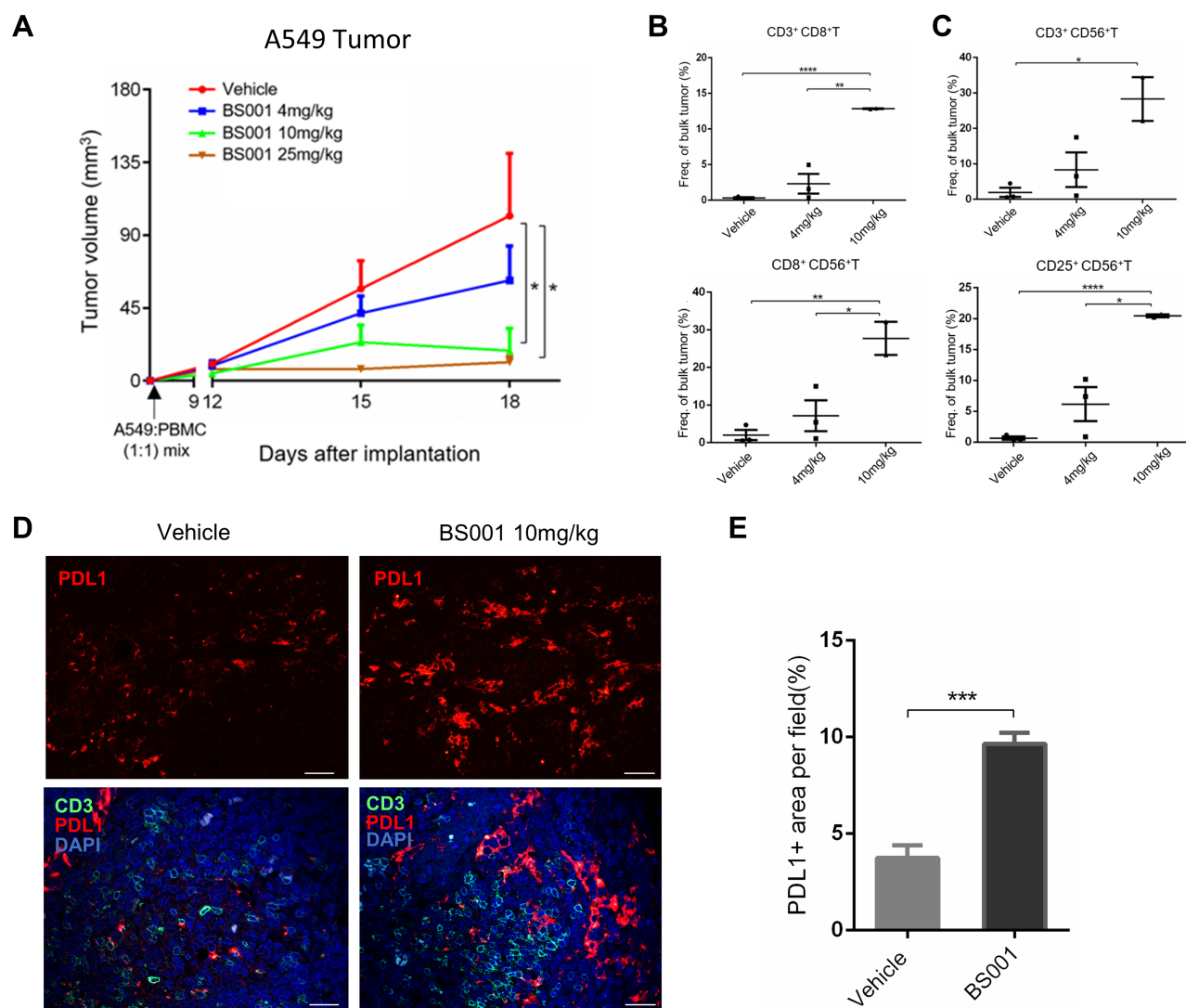


**Figure 5** BS001 inhibits tumor growth in xenograft A549 models.

**Notes:** (A) Tumor volume of treatments with 0, 4, 10, 25 mg/kg BS001 in nude mice. N = 6 for each group. Data were shown as mean  $\pm$  SEM. \* $p$  < 0.05 by two-way ANOVA; (B) Flow cytometry of immune populations from A549 tumors treated dosages of BS001 when stripped on day 18. CD3<sup>+</sup>CD8<sup>+</sup>T cells were stained from the bulk tumor and analyzed by FACS. Data were shown as mean  $\pm$  SEM of three mice from 0, 4mg/kg BS001 and two mice from 10mg/kg group. Most tumors in 1025mg/kg BS001 groups were nearly 100% inhibition and tiny for analysis; (C) Among dissected A549 tumors from different treatments, CD56<sup>+</sup> was detected in infiltrating CD3<sup>+</sup>, CD8<sup>+</sup>, and CD25<sup>+</sup>T cells by FACS. Percentages of CD56<sup>+</sup>T cells in the 0, 4 and 10 mg/kg BS001 groups were calculated and analyzed. The results were shown as mean  $\pm$  SEM. \* $p$  < 0.05, \*\* $p$  < 0.01, \*\*\* $p$  < 0.0001 by unpaired two-tailed *t*-test; (D and E) Immunofluorescence staining analyses of frozen sections revealed infiltrated CD3<sup>+</sup>T cells (green), surrounded by tumor cells expressing high PD-L1 (red) from the 10mg/kg group. Bar:100 $\mu$ m. The results were shown as mean  $\pm$  SEM. \*\*\* $p$  < 0.001 by unpaired two-tailed *t*-test.

**Abbreviations:** FACS, fluorescence-activated cell sorting; PD-L1, programmed cell death protein ligand-1.

## Combination Treatment of BS001 and PD-1/PD-L1 Antibody

Since upregulation of PD-L1 was observed in the tumors treated with BS001, we tested combination therapy of BS001 with PD-L1 antibody to explore whether blocking immune checkpoint PD-1/PD-L1 pathway can enhance anti-tumor efficacy of BS001. At 10 mg/kg of BS001 or 5 mg/kg of anti-PD-L1 antibody, BS001 monotherapy showed modest tumor growth inhibition compared to PBS and PD-L1 group,

respectively ( $p$  < 0.0001) (Figure 6A). Addition to the tumor growth curve, weight of isolated tumors (18 days post treatment, Figure 6B) demonstrated that BS001/anti-PD-L1 combination therapy resulted in more potent tumor inhibition than monotherapies alone ( $p$  < 0.05) (Figure 6C). For drug safe evaluation, the mice in all treatment groups did not show significant body weight reduction (Figure 6D) over the administration period. AST/ALT in mice serum did not change significantly during treatment (Figure S3E). Similar



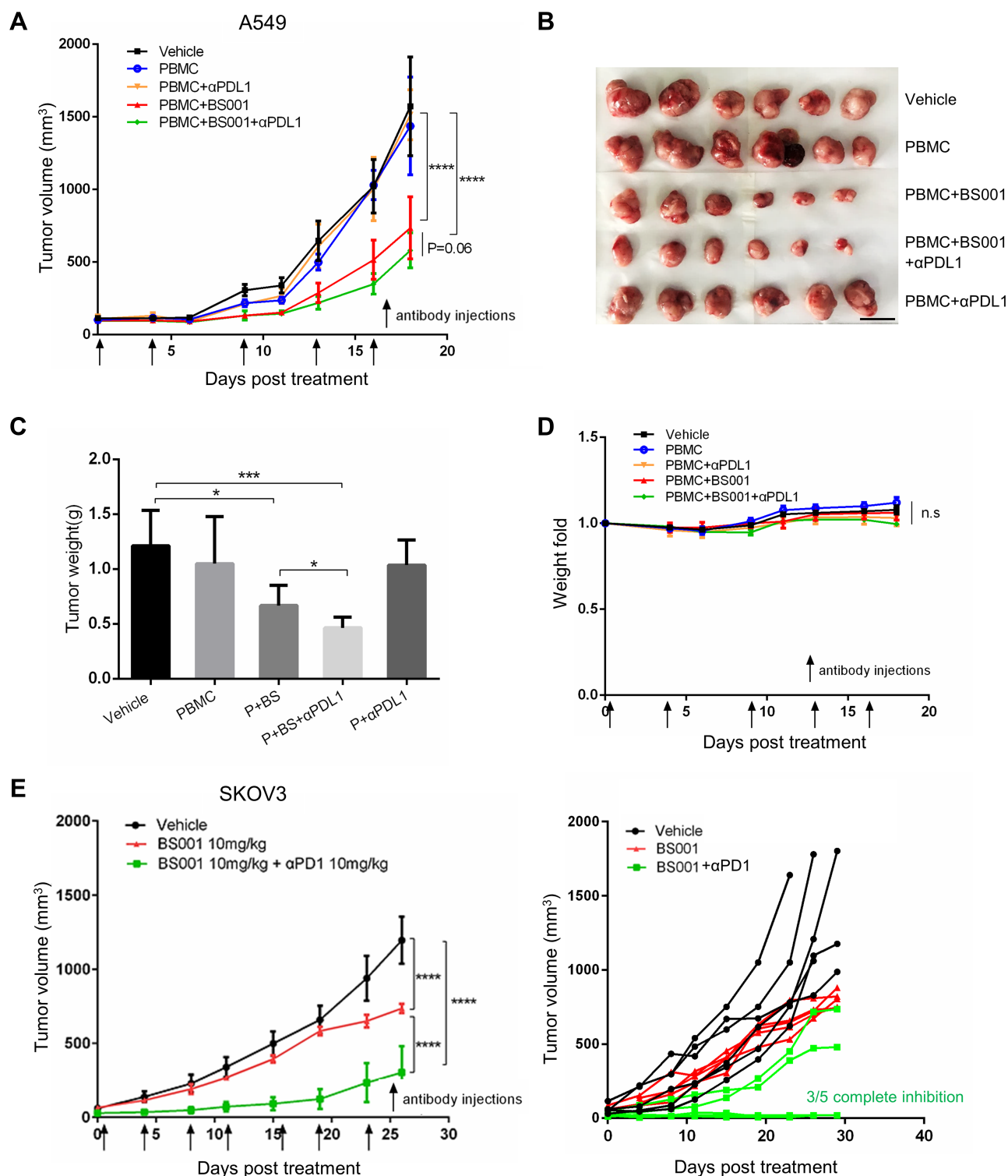


**Figure 6** Combination treatment with BS001 and PD-L1/PD-LI antibody.

**Notes:** (A) In A549, tumor volume measured for treatments with vehicle, BS001, anti-PD-L1 antibody and combination therapy in PBMC-engrafted nude mice on the indicated days. N = 6 for each group. The results were shown as mean  $\pm$  SEM. \*\*\*\* $p$  < 0.0001 by two-way ANOVA; (B) Photograph of dissected tumors from five groups: vehicle, PBMC, PBMC+BS001, PBMC+BS001+ $\alpha$ PD-L1, PBMC+ $\alpha$ PD-L1. Bar:2cm; (C) Weight of dissected tumors from the above five groups. The results were shown as mean  $\pm$  SEM. \* $p$  < 0.05, \*\*\* $p$  < 0.001 by two-tailed t-test; (D) Body weights were measured and fold-changes in all groups were calculated. The results were shown as mean  $\pm$  SEM. n.s, no significant difference; (E) In SKOV3 model, tumor volumes measured on the indicated days, plotted for BS001 treatment, BS001 combined with PD-L1 antibody and control groups. The results were shown as mean  $\pm$  SEM. \*\*\*\* $p$  < 0.0001 by two-way ANOVA

**Abbreviations:** PBMC, peripheral blood mononuclear cell; PD-(L)1, programmed cell death protein (ligand)-1.

results were also seen in the combination therapy of BS001 and PD-1 antibody in SKOV3 model. BS001/anti-PD-1 combination therapy resulted in more potent tumor inhibition than BS001 monotherapies alone. Tumors in 3/5 mice were completely inhibited in the combination therapy group (Figure 6E).

## Discussion

c-Met is an RTK with physiological functions in the normal tissues of mesenchymal origin.<sup>28</sup> Given c-Met's profound roles in cell survival, proliferation, and migration, it is not surprising that this signal pathway is exploited by many tumors and become a common feature of cancer.<sup>29</sup> In this study, we confirmed c-Met over-expression in protein level within all tumor tissues. Our database analysis also showed that *c-Met* gene expression is elevated in transcription level in a variety of tumors. Additionally, c-Met expression on cell surface might be up-regulated after RTK (eg EGFR)-targeted therapy, which often leads to tumor resistance.<sup>30,31</sup> The c-Met expression pattern makes it strong rational for targeted antibody therapy, although several attempts on antibody therapeutics to c-Met have failed.<sup>32–34</sup> Here we explore a bispecific antibody approach to target this tumor surface protein in a different angle.

We designed a novel bispecific antibody that can bind to c-Met and CD3. Each of this antibody molecule can bind to only one CD3 and one c-Met protein targets. This monovalent nature allows the bispecific antibody to avoid undesired activation of T-cells by crossing link CD3 or triggering c-Met signal by receptor dimerization in tumor cells. The structure of CD3 scFv does not affect the binding activity of c-Met in vitro (Figure S1C). This BsAb has a human IgG1 Fc to extend drug half-life time.

Anti-tumor efficacy of this bispecific antibody was demonstrated in both in vitro and in vivo models. In addition, this bispecific antibody has its unique dual mechanisms in tumor killing, besides that it induces T cell-mediated killing by bridging T-lymphocytes and tumor cells, it also inhibits c-Met-phosphorylation by blocking HGF/c-Met interaction. In the clinic, high c-Met phosphorylation levels were seen in many cancers and correlated with poor prognosis.<sup>35</sup> BS001 inhibited HGF-mediated signaling pathway similar to small molecular inhibitor, which could potentially benefit tumor therapy in clinic through combination of BS001 with c-Met-targeting small-molecule drugs to increase efficacy and reduce adversary effects. In

addition to disruption of oncogenic signaling pathways, BS001 can efficiently recruit T cells to kill tumor cells as demonstrated in our in vitro studies. Comparing to the cytotoxicity caused by PBMC, Fc-mediated killing including ADCC effect was very weak by introducing CD3-depleted PBMC as effector cells (Figure S1D). Given the widespread high-expression of c-Met in various tumors, T cell recruiting effect is a novel and more advantageous strategy compared to the mere inhibition of c-Met signal transduction. The cytotoxic potential of the different CD3<sup>+</sup> subsets (CD4<sup>+</sup>, CD8<sup>+</sup>, even NKT) would be informative for the characterization of the cytotoxicity mediated by this antibody. Hence, the dual mechanism of BS001 makes the BS001 a unique modality to provide a new therapy for cancer.

In flow cytometry analyses, BS001 did not show binding activity to murine hepa1-6 or MC38 cancer cells that both expressed murine c-Met (Figure S1E). Since c-Met antibody used in this study is not cross-reactive to murine c-Met, it would be hard to evaluate toxicity evoked by this bispecific antibody in the xenograft model. The cytotoxicity of BS001 on normal c-Met expressing human cells 293T was assessed in vitro, and BS001 showed weak cytotoxicity on 293T as same as MDA-MB-231 (Figure S1F). Future studies were needed to support the safety of the BsAb. As well, the efficacy of BS001 depending on the inhibitory action on c-Met was not properly evaluated in the mouse model. Here, we focused on tumor immunotherapy by CD3 targeting. For solid tumors, it has been a real challenge to achieve clinical efficacy using bispecific antibodies. Many efforts have been made to achieve this goal. Lan et al recently developed trispecific antibodies interacted with CD38, CD3 and CD28 which enhance the therapeutic efficacy of tumor-directed T cells through T cell receptor co-stimulation.<sup>36</sup> Moreover, bispecific antibodies targeting other host immune cells are also under development in several models.<sup>37</sup> For example, CD89 epitope of macrophages and neutrophils,<sup>38,39</sup> CD16 epitope and NKp46 of NK cells.<sup>40,41</sup>

It is an interesting finding that BS001 treatment caused increased PD-L1 expression in lung cancer.<sup>42</sup> IFN- $\gamma$  from lymphocytes induces PD-L1 expression, which might be an explanation to this.<sup>43,44</sup> PD-L1 plays a key role in tumor developing immune evasion to immune surveillance.<sup>45</sup> Immune checkpoint inhibitors such as PD-1/PD-L1 antibodies have been approved to overcome these when treating multiple malignancies; showing remarkable long-term benefit for the patients who respond to the therapy. However, overall patients' response to the immune checkpoint

antibodies was still too low in many types of cancers (eg-10–20%). For those unresponsive patients, combining antibody drugs with different mechanisms might improve the effects of immunotherapy.<sup>46</sup> BS001 and PD-1/PD-L1 antibody combination therapy showed better outcome than monotherapy, which may represent a new option for patients.

## Conclusion

In this study, we designed a novel bispecific antibody BS001 targeting both c-Met and CD3 to potentiate tumor lysis via T cell recruitment. This bispecific antibody can also block c-Met signal transduction. The dual effects of T-cell mediated tumor killing and c-Met signal inhibition may maximize the c-Met-targeted therapy. BS001 exhibited potent anti-tumor efficacy in vitro and in vivo. Combination of BS001 with PD-L1 antibody can further increase therapeutic effect in tumor models.

## Acknowledgments

This study was supported by grants from the National Basic Research Program of China (973 Program) 2015CB553706 and Shanghai Science & Technology Basic Research Program (18JC1414400). The results shown in 1B,1C were based upon data generated by the TCGA Research Network: <https://www.cancer.gov/tcga>. The authors acknowledge the contributions of lab members to the bispecific antibody format design. The authors thank RemeGen, Ltd. for BS001 protein expression.

## Disclosure

Jianmin Fang reports being a shareholder of RemeGen Ltd., outside the submitted work. The authors report no other potential conflicts of interest in this work.

## References

- Peters S, Adjei AA. MET: a promising anticancer therapeutic target. *Nat Rev Clin Oncol*. 2012;9(6):314–326. doi:10.1038/nrclinonc.2012.71
- Furlan A, Kherrouche Z, Montagne R, Copin MC, Tulasne D. Thirty years of research on met receptor to move a biomarker from bench to bedside. *Cancer Res*. 2014;74(23):6737–6744. doi:10.1158/0008-5472.CAN-14-1932
- Smyth EC, Sclafani F, Cunningham D. Emerging molecular targets in oncology: clinical potential of met/hepatocyte growth-factor inhibitors. *Onco Targets Therapy*. 2014;7:1001. doi:10.2147/OTT.S44941
- Dean M, Park M, Le Beau MM, Robins TS, Diaz MO. The human met oncogene is related to the tyrosine kinase oncogenes. *Nature*. 1985;318(6044):385. doi:10.1038/318385a0
- Naldini L, Vigna E, Narsimhan R, Gaudino G, Zarnegar R. Hepatocyte growth factor (hgf) stimulates the tyrosine kinase activity of the receptor encoded by the proto-oncogene c-met. *Oncogene*. 1991;6(4):501–504.
- Maroun CR, Rowlands T. The Met receptor tyrosine kinase: a key player in oncogenesis and drug resistance. *Pharmacol Ther*. 2014;142(3):316–338. doi:10.1016/j.pharmthera.2013.12.014
- Comoglio PM, Giordano S, Trusolino L. Drug development of met inhibitors: targeting oncogene addiction and expedience. *Nature reviews Drug discovery*. *Nat Rev Drug Discov*. 2008;7(6):504. doi:10.1038/nrd2530
- Vigna E, Comoglio PM. Targeting the oncogenic Met receptor by antibodies and gene therapy. *Oncogene*. 2015;34(15):1883–1889. doi:10.1038/onc.2014.142
- Gharwan H, Groninger H. Kinase inhibitors and monoclonal antibodies in oncology: clinical implications. *Nat Rev Clin Oncol*. 2016;13(4):209. doi:10.1038/nrclinonc.2015.213
- Kim K-H, Kim H. Progress of antibody-based inhibitors of the HGF–cMET axis in cancer therapy. *Exp Mol Med*. 2017;49(3):e307. doi:10.1038/emm.2017.17
- Vengoji R, Macha MA, Nimmakayala RK, et al. Afatinib and Temozolomide combination inhibits tumorigenesis by targeting EGFRvIII-cMet signaling in glioblastoma cells. *J Exp Clin Cancer Res*. 2019;38(1):266. doi:10.1186/s13046-019-1264-2
- Rosen LS, Goldman JW, Algazi AP, et al. A first-in-human phase I study of a bivalent MET antibody, emibetuzumab (LY2875358), as monotherapy and in combination with erlotinib in advanced cancer. *Clin Cancer Res*. 2017;23(8):1910–1919. doi:10.1158/1078-0432.CCR-16-1418
- Spigel DR, Ervin TJ, Ramlau RA, et al. Randomized Phase II trial of Onartuzumab in combination with erlotinib in patients with advanced non-small-cell lung cancer. *J Clin Oncol*. 2013;31(32):4105–4114. doi:10.1200/JCO.2012.47.4189
- Merchant M, Ma X, Maun HR, et al. Monovalent antibody design and mechanism of action of onartuzumab, a MET antagonist with anti-tumor activity as a therapeutic agent. *Proc Nat Acad Sci*. 2013;110(32):E2987E2996. doi:10.1073/pnas.1302725110
- Burgess TL, Sun J, Meyer S, et al. Biochemical characterization of AMG 102: a neutralizing, fully human monoclonal antibody to human and nonhuman primate hepatocyte growth factor. *Mol Cancer Ther*. 2010;9(2):400–409. doi:10.1158/1535-7163.MCT-09-0824
- D'Arcangelo M, Cappuzzo F. Focus on the potential role of ficlatuzumab in the treatment of non-small cell lung cancer. *Biologics*. 2013;7:61–68. doi:10.2147/BTT.S28908
- Schlereth, Research BJC.. Eradication of tumors from a human colon cancer cell line and from ovarian cancer metastases in immunodeficient mice by a single-chain Ep-CAM-/CD3-bispecific antibody construct. 2005;65(7):2882–2889. doi:10.1158/0008-5472.CAN-04-2637
- Hirschhaeuser F, Walenta S, Mueller-Klieser W. Efficacy of catumaxomab in tumor spheroid killing is mediated by its trifunctional mode of action. *Cancer Immunol Immunother*. 2010;59(11):1675–1684. doi:10.1007/s00262-010-0894-1
- Wu J, Fu J, Zhang M, Liu D. Blinatumomab: a bispecific T cell engager (BiTE) antibody against CD19/CD3 for refractory acute lymphoid leukemia. *J Hematol Oncol*. 2015;8:104. doi:10.1186/s13045-015-0195-4
- Wang Z, Jensen MA, Zenklusen JC. A practical guide to the cancer genome atlas (TCGA). *Methods Mol Biol*. 2016;1418:111–141.
- Chandrasekar DS, Bashel B, Balasubramanya SAH, et al. UALCAN: a portal for facilitating tumor subgroup gene expression and survival analyses. *Neoplasia*. 2017;19(8):649–658. doi:10.1016/j.neo.2017.05.002
- Nagy A, Lanczky A, Menyhart O, Gyorffy B. Validation of miRNA prognostic power in hepatocellular carcinoma using expression data of independent datasets. *Sci Rep*. 2018;8(1):9227. doi:10.1038/s41598-018-27521-y
- Li H, Chen K, Wang Z, et al. Genetic analysis of the clonal stability of Chinese hamster ovary cells for recombinant protein production. *Mol Biosyst*. 2016;12(1):102–109. doi:10.1039/C5MB00627A

24. Sun Z, Wu Y, Hou W, et al. A novel bispecific c-MET/PD-1 antibody with therapeutic potential in solid cancer. *Oncotarget*. 2017;8(17):29067–29079. doi:10.18632/oncotarget.16173
25. Yin Y, Guo J, Teng F, et al. Preparation of a novel one-armed anti-c-met antibody with antitumor activity against hepatocellular carcinoma. *Drug Des Devel Ther*. 2019;13:4173–4184. doi:10.2147/DDDT.S224491
26. Hsieh Y, Aggarwal P, Cirelli D, et al. Characterization of FcγRIIIA effector cells used in in vitro ADCC bioassay: comparison of primary NK cells with engineered NK-92 and Jurkat T cells. *J Immunol Methods*. 2017;441:56–66. doi:10.1016/j.jim.2016.12.002
27. Lopez-Albaitero A, Xu H, Guo H, et al. Overcoming resistance to Her2-targeted therapy with a novel HER2/CD3 bispecific antibody. *OncoImmunology*. 2017;6(3):e1267891. doi:10.1080/2162402X.2016.1267891
28. Trusolino L, Bertotti A, Comoglio PM. MET signalling: principles and functions in development, organ regeneration and cancer. *Nat Rev Mol Cell Biol*. 2010;11(12):834–848. doi:10.1038/nrm3012
29. Noriega-Guerra H, Freitas VM. Extracellular matrix influencing HGF/c-MET signaling pathway: impact on cancer progression. *Int J Mol Sci*. 2018;19:11. doi:10.3390/ijms19113300
30. Jarantow SW, Bushey BS, Pardinas JR, et al. Impact of cell-surface antigen expression on target engagement and function of an epidermal growth factor receptor x c-MET bispecific antibody. *J Biol Chem*. 2015;290(41):24689–24704. doi:10.1074/jbc.M115.651653
31. Moores SL, Chiu ML, Bushey BS, et al. A novel bispecific antibody targeting EGFR and cMet is effective against EGFR inhibitor-resistant lung tumors. *Cancer Res*. 2016;76(13):3942–3953. doi:10.1158/0008-5472.CAN-15-2833
32. Heukers R, Altintas I, Raghoenath S, et al. Targeting hepatocyte growth factor receptor (Met) positive tumor cells using internalizing nanobody-decorated albumin nanoparticles. *Biomaterials*. 2014;35(1):601–610. doi:10.1016/j.biomaterials.2013.10.001
33. Su Z, Han Y, Sun Q, et al. Anti-MET VHH pool overcomes MET-targeted cancer therapeutic resistance. *Mol Cancer Ther*. 2019;18(1):100–111. doi:10.1158/1535-7163.MCT-18-0351
34. Gherardi E, Birchmeier W, Birchmeier C, Vande Woude G. Targeting MET in cancer: rationale and progress. *Nat Rev Cancer*. 2012;12(2):89–103. doi:10.1038/nrc3205
35. Raghav KP, Wang W, Liu S, et al. cMET and phospho-cMET protein levels in breast cancers and survival outcomes. *Clin Cancer Res*. 2012;18(8):2269–2277. doi:10.1158/1078-0432.CCR-11-2830
36. Wu L, Seung E, Xu L, et al. Trispecific antibodies enhance the therapeutic efficacy of tumor-directed t cells through t cell receptor co-stimulation. *Nature Cancer*. 2019;1–13.
37. Rozan C, Cornillon A, Petiard C, et al. Single-domain antibody-based and linker-free bispecific antibodies targeting FcγRIII induce potent antitumor activity without recruiting regulatory T cells. *Mol Cancer Ther*. 2013;12(8):1481–1491. doi:10.1158/1535-7163.MCT-12-1012
38. Stockmeyer B, Dechant M, van Egmond M, et al. Triggering Fcα-receptor I (CD89) recruits neutrophils as effector cells for CD20-directed antibody therapy. *J Immunol*. 2000;165(10):5954–5961. doi:10.4049/jimmunol.165.10.5954
39. Li B, Xu L, Pi C, et al. CD89-mediated recruitment of macrophages via a bispecific antibody enhances anti-tumor efficacy. *Oncoimmunology*. 2017;7(1):e1380142. doi:10.1080/2162402X.2017.1380142
40. Kipriyanov SM, Cochlovius B, Schafer HJ, et al. Synergistic anti-tumor effect of bispecific CD19 x CD3 and CD19 x CD16 diabodies in a preclinical model of non-Hodgkin's lymphoma. *J Immunol*. 2002;169(1):137–144. doi:10.4049/jimmunol.169.1.137
41. Gauthier L, Morel A, Anceriz N, et al. Multifunctional natural killer cell engagers targeting nkp46 trigger protective tumor immunity. *Cell*. 2019;177(7):1701–1713 e1716. doi:10.1016/j.cell.2019.04.041
42. Sun X, Li C, Wang W, et al. Inhibition of c-MET upregulates PD-L1 expression in lung adenocarcinoma. *Am J Cancer Res*. 2020;10(2):564–571.
43. Martin V, Chiriaco C, Modica C, et al. Met inhibition revokes IFNγ-induction of PD-1 ligands in MET-amplified tumours. *Br J Cancer*. 2019;120(5):527–536. doi:10.1038/s41416-018-0315-3
44. Abiko K, Matsumura N, Hamanishi J, et al. IFN-γ from lymphocytes induces PD-L1 expression and promotes progression of ovarian cancer. *Br J Cancer*. 2015;112(9):1501–1509. doi:10.1038/bjc.2015.101
45. Woo SR, Turnis ME, Goldberg MV, et al. Immune inhibitory molecules LAG-3 and PD-1 synergistically regulate T-cell function to promote tumoral immune escape. *Cancer Res*. 2012;72(4):917–927. doi:10.1158/0008-5472.CAN-11-1620
46. Chang CH, Wang Y, Li R, et al. Combination therapy with bispecific antibodies and PD-1 blockade enhances the antitumor potency of T cells. *Cancer Res*. 2017;77(19):5384–5394. doi:10.1158/0008-5472.CAN-16-3431

## Drug Design, Development and Therapy

Dovepress

## Publish your work in this journal

Drug Design, Development and Therapy is an international, peer-reviewed open-access journal that spans the spectrum of drug design and development through to clinical applications. Clinical outcomes, patient safety, and programs for the development and effective, safe, and sustained use of medicines are a feature of the journal, which has also

been accepted for indexing on PubMed Central. The manuscript management system is completely online and includes a very quick and fair peer-review system, which is all easy to use. Visit <http://www.dovepress.com/testimonials.php> to read real quotes from published authors.

Submit your manuscript here: <https://www.dovepress.com/drug-design-development-and-therapy-journal>